Check for updates

JGR Earth Surface

RESEARCH ARTICLE
10.1029/2025JF008718

Linked Canyons and Fans Communicate Through a Migrating Bedrock-Alluvial Transition

Li Zhang[1], Gary Parker[2], Jeffrey Nittrouer[3], Xudong Fu[4], Shanghong Zhang[1], and Guangqian Wang[4]

[1]School of Water Resources and Hydropower Engineering, North China Electric Power University, Beijing, China, [2]Department of Earth Science & Environmental Change and Department of Civil & Environmental Engineering, University of Illinois Urbana-Champaign, Urbana, IL, USA, [3]Department of Geosciences, Texas Tech University, Lubbock, TX, USA, [4]Department of Hydraulic Engineering, Tsinghua University, Beijing, China

Key Points:

- The bedrock-alluvial transition point in a canyon-fan system may be located within the canyon itself, and not at the canyon mouth
- This state can arise as alluvium covers the canyon bedrock basement and turns off incision, even when the system is tectonically active
- The bedrock-alluvial transition is pushed to the canyon-valley mouth only when the rate of production of accommodation is large

Supporting Information:

Supporting Information may be found in the online version of this article.

Correspondence to:

L. Zhang and G. Parker,
53802829@ncepu.edu.cn;
parkerg@illinois.edu

Citation:

Zhang, L., Parker, G., Nittrouer, J., Fu, X., Zhang, S., & Wang, G. (2026). Linked canyons and fans communicate through a migrating bedrock-alluvial transition. *Journal of Geophysical Research: Earth Surface*, *131*, e2025JF008718. https://doi.org/10.1029/2025JF008718

Received 27 JUL 2025
Accepted 1 JUN 2026

© 2026. The Author(s).
This is an open access article under the terms of the Creative Commons Attribution License, which permits use, distribution and reproduction in any medium, provided the original work is properly cited.

Abstract Net-erosional fluvial landscapes are often treated separately from net-depositional fluvial landscapes. Yet these landscapes are often tightly linked by means of a moving-boundary bedrock-alluvial transition. We consider a linked canyon-fan system in a Basin and Range province, basing our work loosely on Rainbow Canyon and Panamint Valley, USA. The canyon is mixed bedrock-alluvial upstream, and incises into a plateau undergoing uplift. The fan is purely alluvial, and is part of a bajada in the adjacent valley undergoing subsidence. It might be thought that uplift would push the bedrock-alluvial transition out to the canyon mouth. Yet this transition is often observed to be well up the canyon itself. Here we show that this does not necessarily indicate that the region is tectonically quiescent. The migration of this transition can be explained in terms of canyon-fan interaction captured by a single, dimensionally homogeneous morphodynamic model which folds in alluvial and incisional processes.

Plain Language Summary A Basin and Range province is a succession of parallel uplifting mountain ranges and subsiding valleys. Each canyon forms at a right angle to the range, cuts into the uplifting mountains and sends sediment to the connected subsiding depositional fan in the valley just downstream. Canyon and fan talk to each other through a moving boundary transition. The channel is bedrock-alluvial upstream of this boundary and purely alluvial (loose sediment deposited by flowing water) downstream. We show that this transition point need not be at the canyon mouth, but can migrate upstream into the canyon itself, even in the presence of active uplift. Alluviation on top of the canyon basement cuts off incision, reduces storage space for sediment above it, and pushes the bedrock-alluvial transition point upstream faster than otherwise. When the rate of production of accommodation (available space in which sediment can be stored through deposition) due to subsidence in the valley is sufficiently high, however, the transition can migrate to the canyon mouth, in some cases creating a vertical step expressed as a waterfall.

1. Introduction

Steep, narrow canyons often link to wide alluvial fans (Blair & McPherson, 2009). The canyon is often bedrock-dominated, whereas the fan is alluvial. Here we use "Bedrock" as shorthand for "mixed bedrock-alluvial" (Sklar & Dietrich, 2004, 2006). We consider a linked canyon-fan system in a Basin and Range province such as the southwestern United States. Such provinces consist of subparallel mountain ranges undergoing relative uplift bounding valleys undergoing relative subsidence, corresponding to alternating horsts and grabens produced by deep-seated tectonic extension (Stewart, 1971). A series of canyons perpendicular to the range crest incise into the mountains, each emptying to a fan. The fans often amalgamate to form a bajada. Basin and Range topography is not unique to the southwestern United States; two other examples are in east Asia (Mongolian Plateau, Windley & Allen, 1993; Eastern NE Asia, Zhou et al., 2023).

We consider the morphodynamics of a single linked canyon-fan system, loosely based on Rainbow Canyon and its fan within the Panamint Valley bajada, Death Valley National Park, USA (Waskiewicz et al., 2008). Figure 1a shows the region that motivates our study, including the Argus Range and Panamint Valley. Figure 1b shows the V-shaped Rainbow Canyon. Figure 1c shows the canyon, fan, and present location of the bedrock-alluvial transition. Figure 1d is a definition diagram for our simplified morphodynamic model, in which Santa Rosa Wash is the alluvial feeder channel from Darwin Plateau in the Argus range, B_c = width of the canyon channel (also taken to be the width of a virtual channel that migrates and avulses across the valley deposit as shown in

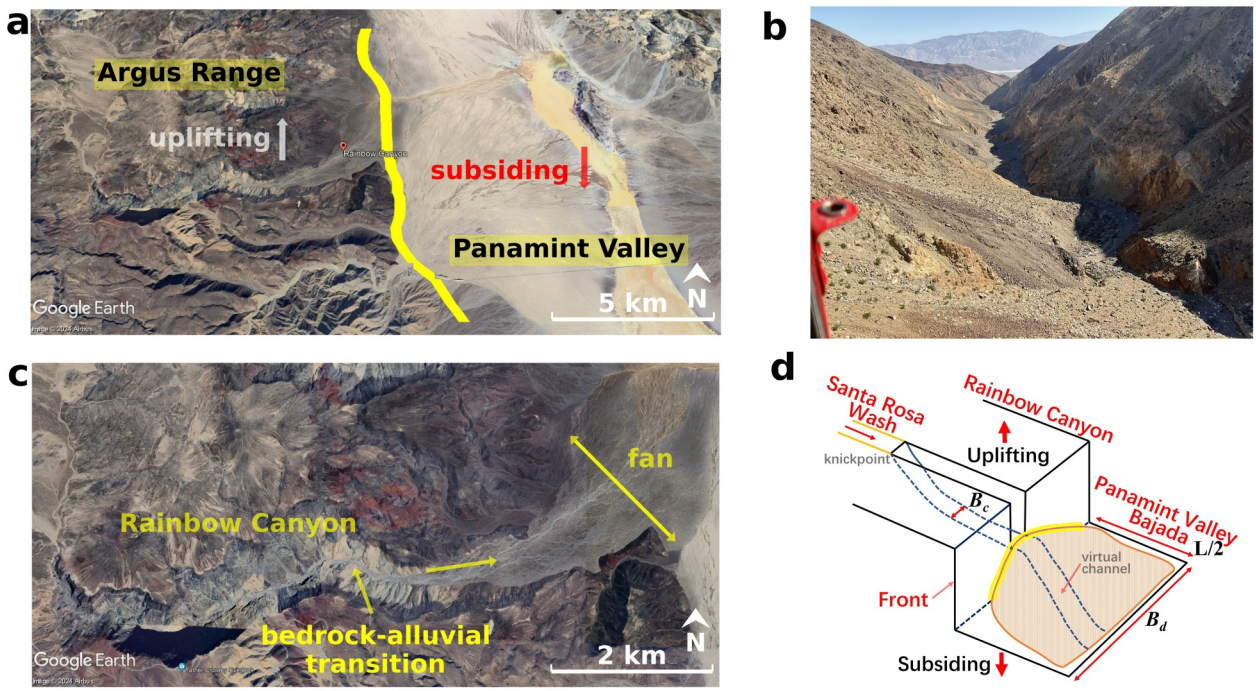

Figure 1. Setting for Rainbow Canyon and its corresponding fan in Panamint Valley. (a) The Argus Range and Panamint Valley showing the front line between the two (yellow line). The mouth of the canyon is at (36°22′24.34″N, 117°29′23.90″W). (b) Helicopter view of Rainbow Canyon looking upstream on 22 October 2023. (c) Rainbow Canyon and its corresponding fan, showing the position of the bedrock-alluvial transition upstream of the canyon mouth. (d) Definition diagram for a simplified model of the canyon-fan system; B_c denotes bottom canyon width, which also equals the width of the virtual channel in the valley, B_d denotes the valley depositional width and L denotes the length parallel to the canyon from the initial canyon head to the downstream end of the valley.

Figure 1d), B_d = width of the depositional zone corresponding to valley depositional width, equal to fan width in this simplified model, and L = initial length of the initial canyon-fan system, evenly split between canyon and fan. The length of the canyon subreach can change as a plateau-canyon knickpoint migrates upstream. Sediment is supplied from Darwin Plateau beyond the canyon head. The watershed extends upstream into the Argus Range (Zhang et al., 2020). The canyon head (knickpoint) is characterized by three incisional cyclic steps (Scheingross et al., 2019, 2020; Scheingross & Lamb, 2017). The canyon itself is V-shaped lacking tributaries (Figure 1b).

Bedrock-alluvial transitions are commonly observed where mountains give way to plains. Two examples are the Fall Line, eastern United States, marking the boundary between the Appalachian Piedmont and the coastal plain (Hupp, 2000; Pavich, 1989) and Yumenkou (Sun et al., 2022) where the Yellow River flows off of the Loess Plateau, China. Bedrock-alluvial transitions can correspond to divides in plant species type (Nucci et al., 2012). Figure 1c shows that in the case of Rainbow Canyon the bedrock-alluvial transition occurs not at the canyon mouth, where a front bounds uplifting and subsiding zones, but approximately halfway up the canyon (verified by a helicopter survey by the authors on 22 October 2023 and a ground survey by the authors on 18-19 January 2024). Relevant length scales are given in Figures 1a and 1c. Multiple examples of this pattern, with a wide multiple-channel depositional zone at the canyon mouth constricting to a very narrow single-channel zone upcanyon, can be inferred though an inspection of adjacent channels flowing off the Argus Range and the adjacent Panamint Range using Google Earth. This feature presents a conundrum: in so far as alluvial cover precludes the balancing of uplift by incision and uplift continues upstream of the bedrock-alluvial transition, why does the uplifting mountain range not push the transition to the canyon mouth?

Experiments and morphodynamic modeling are powerful tools to study canyon-fan evolution. Morphodynamic models can link hydraulics, sediment transport, alluviation and incision to describe system evolution. Features such as tectonics, base level change and abrasion can be included. Experimental and field results have been used to verify morphodynamic models of alluvial fans and fan-deltas (Parker et al., 1998a, 1998b; Sun et al., 2002; Whipple et al., 1998). Cellular models have been used to study linked uplands (including canyons) and fans (Densmore et al., 2007; Pepin et al., 2010; Welivitiya et al., 2020). These models do not, however, focus on the

21699011, 2026, 6, Downloaded from https://agupubs.onlinelibrary.wiley.com/doi/10.1029/2025JF008718 by Texas Tech University Libraries, Wiley Online Library on [30/09/2026]. See the Terms and Conditions (https://onlinelibrary.wiley.com/terms-and-conditions) on Wiley Online Library for rules of use; OA articles are governed by the applicable Creative Commons License

dynamics of a bedrock-alluvial transition. Bedrock-alluvial transitions have been modeled experimentally (Kim et al., 2013; Kim & Muto, 2007; Muto, 2001; Muto & Steel, 2001). Numerical models motivated in part by this work can reproduce the dynamics of migrating bedrock-alluvial transitions observed at experimental and field scale (Jafarinik & Viparelli, 2020; Parker et al., 2008a, 2008b; Viparelli et al., 2015). None of these models incorporates bedrock incision.

Bedrock incision has been modeled using the stream power model, where the incision rate is linked to channel slope and upstream drainage area (Howard, 1994; Whipple & Tucker, 1999). While useful for many purposes in original and extended form (Gasparini & Brandon, 2011; Lague, 2014), the original form does not incorporate sediment transport dynamics, and thus cannot be straightforwardly linked to a depositional zone. The first model of incisional bedrock channels that incorporates sediment transport dynamics appears to be the Saltation-Abrasion model (Chatanantavet & Parker, 2008, 2009; Sklar & Dietrich, 2004, 2006), according to which incision occurs only when the bedrock has a partial cover of alluvium (Sklar & Dietrich, 2004; Turowski et al., 2007). The Saltation-Abrasion model captures bedrock incision mediated by particles striking the bedrock surface. It can be linked to the Exner equation of sediment conservation to describe spatiotemporal morphodynamic evolution, as in the case of a model of incisional morphodynamics of a simplified configuration based on Rainbow Canyon (Zhang et al., 2020). That model, however, is not linked to a fan downstream.

Here we present a single morphodynamic model incorporating (a) alluvial morphodynamics using a standard sediment transport equation and the Exner equation of sediment conservation, (b) incisional morphodynamics including below-capacity sediment transport mediated by the fraction of bedrock surface area p covered by alluvium, (c) simplified tectonics (uplift and incision without extension), (d) upstream knickpoint migration at the channel head, (e) sediment from sidewall erosion, and (f) a downstream boundary condition for either a closed or open basin. The bedrock-alluvial transition point is not assumed, but rather captured in the numerical model where the cover fraction changes from $p < 1$ to $p = 1$.

2. Configuration, Morphodynamic Model and Input Parameters

Our formulation for incision is based on the Saltation-Abrasion model of Sklar and Dietrich (2004). The model itself is a point model which cannot be used directly for morphodynamics. Zhang et al. (2015) adapted this formulation for morphodynamic calculations in terms of the Macro-Roughness-based Saltation-Abrasion-Alluviation (MRSAA) model. Zhang et al. (2020) further developed it for canyon evolution in terms of the Moving-boundary Panamint Incision by Gravel Grinding (MOVING-PIGG) formulation. Here we add a purely depositional zone (fan, or more precisely bajada) to the formulation. The governing equations described in Text S1 of Supporting Information S1 constitute a unified model capturing canyon-fan morphodynamic interaction. Relevant caveats are listed there.

Our configuration is a highly simplified version of the Rainbow Canyon-Panamint fan system of Figure 1d. The system itself is a half graben with a complicated tectonic history (Burchfiel et al., 1994; Cichanski, 2000); for simplicity we consider here a full graben with a subsiding valley (loosely corresponding to Panamint Valley) and an uplifting mountain range (loosely corresponding to the Argus Range). We include (a) a plateau with slope S_p toward Panamint Valley (loosely corresponding to Darwin Plateau in the Argus Range) uplifting at a constant rate υ, (b) a non-incising feeder channel (Santa Rosa Wash) and an upstream-migrating canyon knickpoint, (c) a V-shaped canyon with constant side slope S_s and initial length $L/2$, no tributaries and an incising canyon bottom with constant width B_c, (d) a front dividing the plateau and the valley (Figure 1a), (e) a valley basement subsiding at constant rate σ, (f) an alluvial valley depositional zone (corresponding to the fan) of valley depositional width B_d and constant length $L/2$, and (g) a virtual channel on the deposit of the same width B_c as the canyon, but which implicitly spreads sediment deposits across the fan surface via migration-avulsion (Parker et al., 1998a, 1998b; see Figure 1d). Valley subsidence creates accommodation (available space in which sediment can be stored through deposition), the volume rate of creation of which is given by valley surface area times the subsidence rate. Flood flows are intermittent, with constant flood discharge Q_w occurring at constant time fraction I_f. Where x is distance downstream of the initial position of the canyon head (which is a knickpoint initially at $x = 0$ km but which migrates upstream), the uplifting canyon extends to $x = L/2$, and the subsiding valley extends from $x = L/2$ to L. Canyon and valley slopes are S_c and S_v respectively; and their initial values are S_{ci} and S_{vi}. Finally x_{ba} denotes the position of the bedrock-alluvial transition.

21699011, 2026, 6, Downloaded from https://agupubs.onlinelibrary.wiley.com/doi/10.1029/2025JF008718 by Texas Tech University Libraries, Wiley Online Library on [30/09/2026]. See the Terms and Conditions (https://onlinelibrary.wiley.com/terms-and-conditions) on Wiley Online Library for rules of use; OA articles are governed by the applicable Creative Commons License

21699011, 2026, 6, Downloaded from https://agupubs.onlinelibrary.wiley.com/doi/10.1029/2025JF008718 by Texas Tech University Libraries, Wiley Online Library on [30/09/2026]. See the Terms and Conditions (https://onlinelibrary.wiley.com/terms-and-conditions) on Wiley Online Library for rules of use; OA articles are governed by the applicable Creative Commons License

Table 1
Values of Set Parameters in the Present Study

Parameter	Value	Notes
Q_w, m^3/s	29	Flood discharge
I_f	0.005	Flood intermittency fraction
D, mm	60	Grain size
B_c, m	20	Canyon bottom width
Cz	10	Chezy resistance coefficient
q_{af}, m^2/s	0.00134	Computed volume sediment transport rate/width during floods for prevailing conditions in Santa Rosa Wash
L, km	8	$L/2$ = initial length of canyon and $L/2$ = length of valley
β, km^{-1}	0.015	Abrasion coefficient for incision relation
λ	0.35	Porosity of alluvium
S_s	0.7	Canyon sidewall slope
S_{ci}	0.094	Initial canyon slope
S_{vi}	0.047	$=S_{ci}/2$, initial valley slope
S_p	0	Plateau slope

Other parameters include elevation of the bedrock surface η_b, thickness of the alluvial layer η_a above it, bed elevation $\eta = \eta_b + \eta_a$, areal fraction cover of alluvium over the bedrock surface p, bedrock incision rate E, grain size D of the gravel alluvium, submerged specific gravity R of the gravel particles, bed slope $S = -\partial\eta/\partial x$, dimensionless Chezy bed friction coefficient Cz, volume transport rate per unit width of sediment q_a, capacity sediment transport rate per unit width q_{ac}, upstream sediment feed rate q_{af}, bedrock abrasion coefficient β used in the relation for incision, and fraction f_b of failed material from canyon sidewalls that remains as competent gravel on the canyon bottom and deposit porosity λ. All symbols are defined in the Table of Symbols and Values given in Text S2 of Supporting Information S1. Parameters with values that are common to all the runs are given in Table 1. These are largely based on previous work (Labotka & Albee, 1990; Zhang et al., 2020). Input parameters varied in the calculations are: the subsidence rate of the valley σ (0–3 mm/year), uplift rate of the canyon υ (0–5 mm/year), valley depositional width B_d (100–800 m) and fraction f_b of material eroded from the canyon walls that is retained as competent gravel in the channel (0–0.5). We specify the ratio $r = B_d/B_c$ rather than B_d itself (the former with the range 1–40). The other parameters listed above are either specified or calculated based on the formulation in Text S1 of Supporting Information S1. The range of values of uplift rate υ used here center on the value $\upsilon = 3$ mm/year, based on the estimate of 120 m of uplift of the Panamint Range over the most recent 40,000 years (Labotka & Albee, 1990). Downstream boundary conditions include (a) free below-capacity outflow from basin (Zhang et al., 2018) and (b) closed basin, according to which the sediment transport rate vanishes at the downstream end of the valley. Relevant parameters pertaining to the model configuration are defined in Figures 1d and 2. Details concerning boundary conditions are specified in Text S1 of Supporting Information S1.

3. Morphodynamics of Pure Incision and Pure Alluviation

Our goal is the morphodynamics of the bedrock-alluvial transition in a linked system of an uplifting canyon and subsiding fan. Before proceeding, we study model behavior under simpler conditions of pure incision and pure alluviation.

Results for pure incision are shown in Figures 3a and 3b. In both cases the downstream "fan" (lower reach) is not actually a fan, but is instead a continuation of the canyon (upper reach) at half the initial canyon slope S_{ci}. The upper and lower reaches have the same width ($r = 1$), so that valley depositional width B_d = canyon width B_c. As outlined in Text S1 of Supporting Information S1, the incision rate E in the upper reach is set at 3 mm/year. A somewhat lower value of incision rate prevails in the lower reach due to lower slope but a below-capacity sediment transport rate equal to that of the upper reach. The downstream boundary condition is one of free below-capacity sediment outflow. Sidewall erosion is assumed to contribute no competent gravel to the bed, so $f_b = 0$.

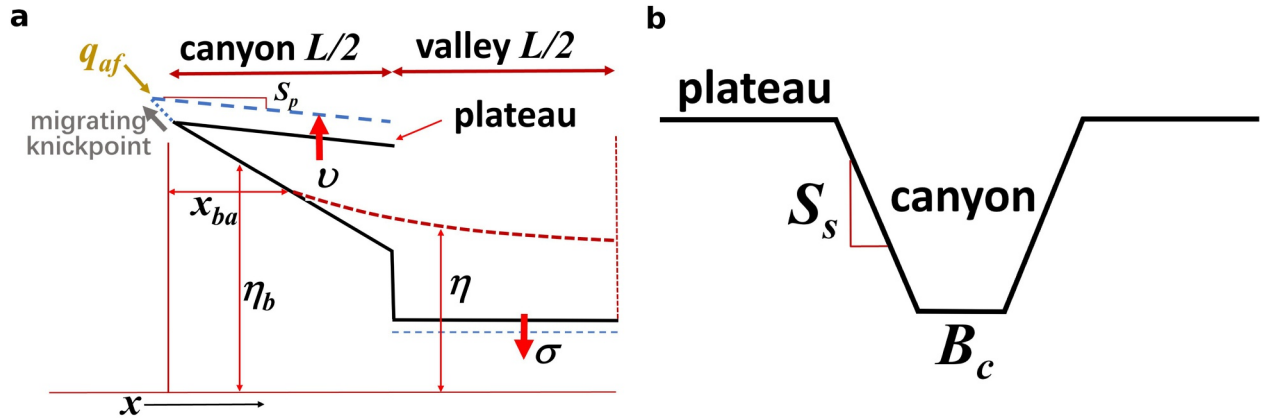

Figure 2. Definition diagram for several of the parameters in the model configuration. a, Long profile of the canyon-valley centerline. b, Canyon cross-section. Here x = streamwise coordinate, x_{ba} = position of bedrock-alluvial transition, υ = plateau uplift rate, σ = valley subsidence rate, η = bed elevation, η_b = elevation to top of bedrock, q_{af} = volume feed rate of alluvial gravel per unit width, $L/2$ = streamwise length of valley and initial streamwise length of canyon, S_p = plateau slope, S_s = side slope of canyon and B_c = width of canyon bottom.

In Figure 3a, the uplift rate $\upsilon = 5$ mm/year. Uplift outpaces the incision rate $E = 3$ mm/year everywhere, so bedrock elevation η_b increases over time, and the knickpoint migrates upstream at a slope that is higher than the upstream reach. In Figure 3b uplift rate $\upsilon = 0.5$ mm/year; incision outpaces uplift, bedrock elevation everywhere decreases over time, and the knickpoint migrates upstream at a slope that is lower than the upstream reach. Under pure incision, bedrock slope remains temporally constant at its initial value. Were the uplift rate set equal to the incision rate of 3 mm/year and the lower reach have the same slope as the upper reach, nothing would change in time other than the upstream migration of the knickpoint. This is case is illustrated for the upper reach in Figure S1 of Supporting Information S1.

Results for pure alluviation are shown in Figure 3c. The calculation of Figure 3c is extended in time in Figure 3d. Tectonics are turned off, so that $E = \upsilon = \sigma = 0$, and also $f_b = 0$. The bedrock basement remains fixed with the lower reach having half the slope of the upper reach, and $r = 1$. The downstream boundary condition is such that all sediment is captured (zero outflow; closed basin). Figure 3c shows elevation of the top of the alluvium η up to 1600 years. Alluvium is seen to passively onlap the bedrock basement. Figure 3d shows a continuation of the calculation of Figure 3c until alluvium spills onto the plateau. The spatiotemporal evolution of cover factor p corresponding to Figures 3c and 3d are shown in Figures 3e and 3f, respectively.

4. Morphodynamics of the Bedrock-Alluvial Transition as the Canyon and Fan Interact With Each Other in a Basin and Range Setting

We now capture canyon-fan interaction where the canyon uplifts and the valley subsides. As in Figures 3a and 3b, upper-reach parameters are set so the bedrock incises at $E = 3$ mm/year wherever exposed. The fan (lower reach) subsides at $\sigma = 3$ mm/year in all cases, and $r = 5$, so the fan is 5 times wider than the canyon. The canyon (upper reach) uplifts at rates $\upsilon = 0$, 3 and 5 mm/year. Sidewall failure does not produce competent gravel, that is, $f_b = 0$.

Figure 4a–4c show bedrock elevation η_b and elevation η of top of the alluvium after 24,000 years for the base cases $\upsilon = 3$ mm/year and the variant cases 0 mm/year and 5 mm/year. In Figure 4d, the three results are superimposed. These figures show three features capturing how the canyon and valley communicate with each other. (a) For the case $\upsilon = 3$ mm/year (Figure 4a), onlapping of alluvium top the bedrock turns off incision in the canyon, so that bedrock elevation rises downstream of the bedrock-alluvial transition. Uplift and incision balance upstream of this transition, so bed elevation does not change there. Onlapping onto the bedrock causes cessation of incision. The loss of accommodation due to this cessation is shown in blue, and the remaining, reduced accommodation is shown in yellow. The loss of accommodation drives the bedrock-alluvial transition upstream faster than otherwise. (b) A comparison of Figures 4a and 4b shows that vanishing uplift does not give rise to concomitant loss in accommodation, but a similar comparison of Figures 4a and 4c shows that increased uplift exacerbates the loss in accommodation. (c) Figure 4d shows that at 24,000 years, increasing uplift rate pushes the streamwise position x_{ba} of the bedrock-alluvial transition valleyward, indicating strong canyon-valley

21699011, 2026, 6, Downloaded from https://agupubs.onlinelibrary.wiley.com/doi/10.1029/2025JF008718 by Texas Tech University Libraries, Wiley Online Library on [30/09/2026]. See the Terms and Conditions (https://onlinelibrary.wiley.com/terms-and-conditions) on Wiley Online Library for rules of use; OA articles are governed by the applicable Creative Commons License

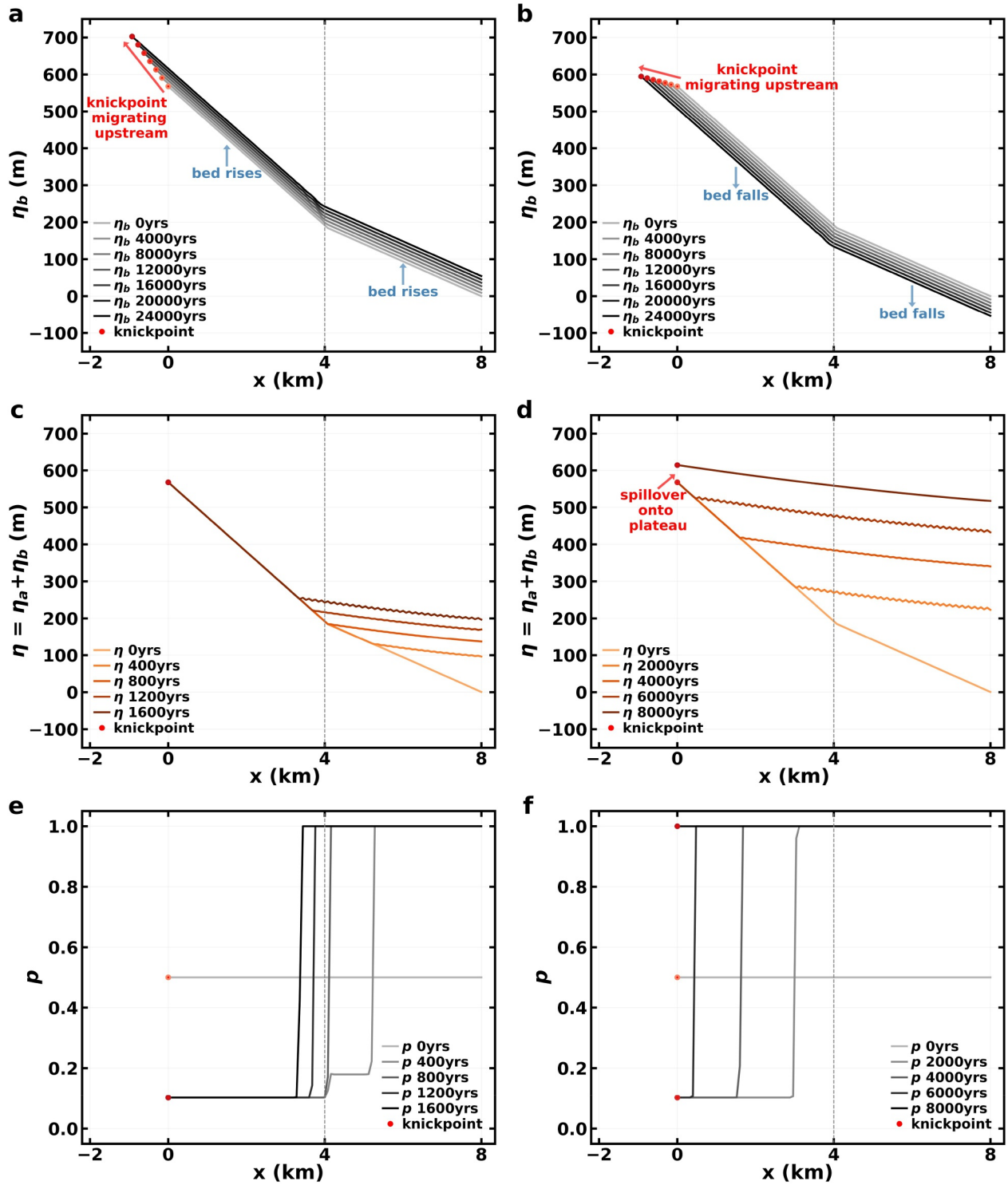

Figure 3. Behavior for pure incision and pure alluviation. (a) Case of pure incision; no fan, slope $S_c = S_{ci} = 0.094$ for upper reach and slope $S_v = S_{vi} = 0.047$ for lower reach, $r = 1$, incision rate $E = 3$ mm/year for upper reach and 2.74 mm/year for lower reach (corresponding to the same sediment transport rate as upstream but half the slope), uplift rate $\upsilon = 5$ mm/year everywhere. (b) Case of pure incision; again no fan, all parameters identical to Case a (i.e., Figure 3a) except $\upsilon = 0.5$ mm/year everywhere. (c) Case of pure alluviation; slope $S_{ci} = 0.094$ for upper reach and $S_{vi} = 0.047$ for lower reach, $r = 1$, $E = \upsilon = \sigma = 0$. (d) Same as Case c, but calculation continued until sediment spills onto plateau. (e) Spatiotemporal variation in cover factor p corresponding to Case c. (f) Spatiotemporal variation of cover factor p corresponding to Case d. In Figures 3c and 3d, the elevation of the bedrock basement η_b is always only slightly below the bed surface elevation η at 0 years. In both Cases c, d the initial value of cover factor p was set to 0.5, as shown by the horizontal lines in Figures 3e and 3f. The value of p near 0.1 upstream of the migrating bedrock-alluvial transition apparent in panels e and f indicates D that alluvium is available to actively incise the bedrock there.

21699011, 2026, 6, Downloaded from https://agupubs.onlinelibrary.wiley.com/doi/10.1029/2025JF008718 by Texas Tech University Libraries, Wiley Online Library on [30/09/2026]. See the Terms and Conditions (https://onlinelibrary.wiley.com/terms-and-conditions) on Wiley Online Library for rules of use; OA articles are governed by the applicable Creative Commons License

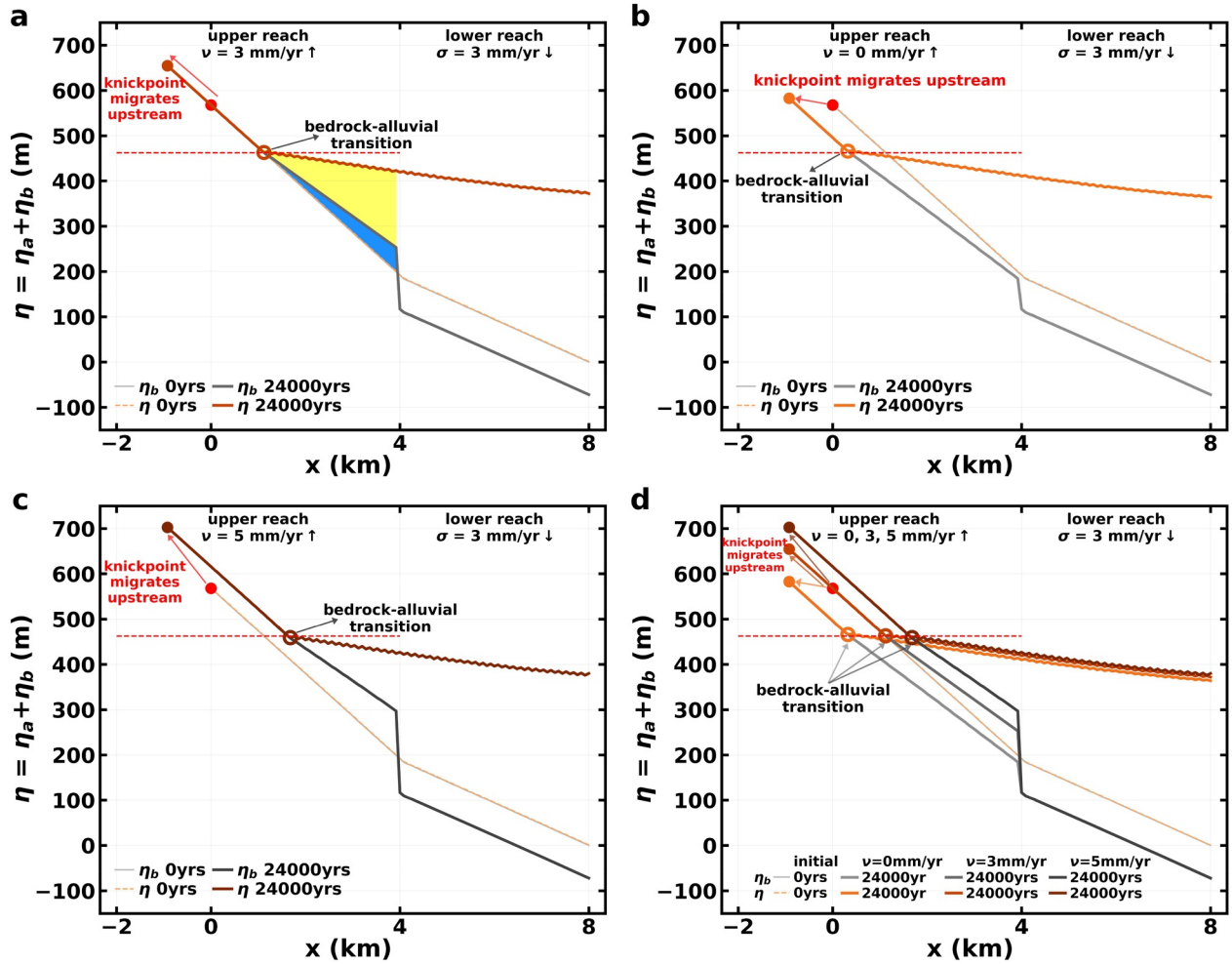

Figure 4. Behavior for canyon-fan interaction showing the time evolution of the partially exposed bedrock reach, the alluviated bedrock basement reach, the top of the alluvial cover, the bedrock-alluvial transition and the upstream knickpoint. In all cases $r = 5$, $\sigma = 3$ mm/year, $E = 3$ mm/year wherever bedrock is exposed and $f_b = 0$. (a) $\upsilon = 3$ mm/year. (b) $\upsilon = 0$ mm/year. (c) $\upsilon = 5$ mm/year. (d) Cases a–c plotted together. Note that the streamwise position of the bedrock-alluvial transition is displaced valleyward with increasing uplift rate, but the elevation of this transition remains constant. The result concerning streamwise position and elevation generalizes to times other than the maximum time of 24,000 years shown here.

communication. The elevation η_{ba}, however remains invariant. This evidently implies a balance between the effect of net rise or fall of the bedrock reach upstream of the transition and net loss of accommodation as alluviation turns off incision below the deposit. Although results are shown for only 24000 years for clarity, they generalize for earlier and later times with the restrictions that (a) the valley floor is no longer exposed and (b) the alluvium has not yet spilled onto the plateau.

Figure 5a shows a plot of η_{ba} and x_{ba} versus uplift, generalizing the results of Figure 4 to the five uplift rates $\upsilon = 0$–5 mm/year. It is seen that the elevation of the bedrock-alluvial transition remains constant with uplift rate. Increasing uplift rate, however, pushes the position of the bedrock-alluvial transition valleyward, but not into the valley itself. This raises the question as to whether any rate of canyon uplift or creation of valley accommodation is sufficient to keep alluvium from onlapping the canyon floor. This issue is explored in Figure 5b. All model conditions are the same as for Figure 4a, except r is increased from 5 to 10, 20, and finally to 40. The valley depositional width, which corresponds to the width of accommodation of the fan thus increases from 100 to 800 m. It is seen that the wider the surface over which sediment is deposited (valley depositional width), the less efficiently is the accommodation created by subsidence filled with sediment. The creation rate of accommodation due to subsidence in the widest valley is so large that an uplift rate of 3 mm/year is sufficient to ensure that

21699011, 2026, 6, Downloaded from https://agupubs.onlinelibrary.wiley.com/doi/10.1029/2025JF008718 by Texas Tech University Libraries, Wiley Online Library on [30/09/2026]. See the Terms and Conditions (https://onlinelibrary.wiley.com/terms-and-conditions) on Wiley Online Library for rules of use; OA articles are governed by the applicable Creative Commons License

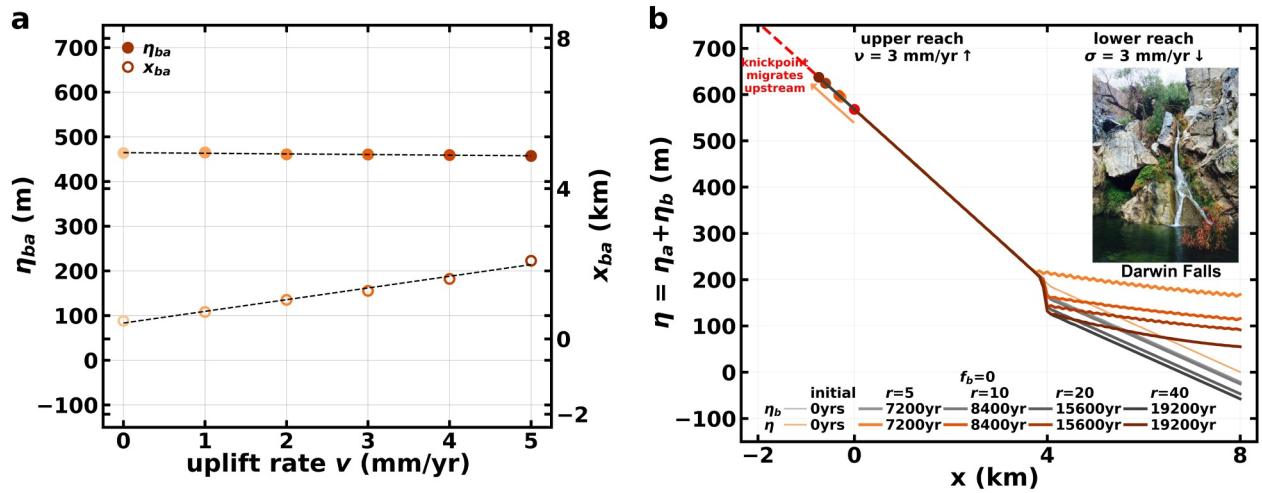

Figure 5. Illustration of communication between canyon and valley fan, or lack thereof. (a) Streamwise position x_{ba} and elevation η_{ba} of the bedrock-alluvial transition at 24000 years for valley subsidence rate $\sigma = 3$ mm/year, bedrock incision rate $E = 3$ mm/year when exposed, uplift rate v varies from 0 to 5 mm/year and ratio r of valley depositional width to canyon width = 5. The variation of x_{ba} with v is indicative of strong communication between canyon and valley. Elevation at the bedrock-alluvial transition η_{ba}, however, remains independent of v. (b) Calculational conditions are the same as Figure 4a ($\sigma = v = E = 3$ mm/year), and no sidewall feed ($f_b = 0$) for all the four cases $r = 5$, 10, 20, and 40. The calculation results are at 7200 years for $r = 5$, at 8400 years for $r = 10$, at 15600 years for $r = 20$, and at 19200 years for $r = 40$ separately. The results indicate that the wider the valley, the less effective alluvium is at filling the accommodation created by subsidence. Under the conditions $r = 10$, 20, and 40 the canyon and valley no longer communicate with each other after certain time. The threshold value for this transition is close to $r = 9$. Beyond this transition a vertical knickpoint, or waterfall forms. The case of Darwin Falls, two canyons south of Rainbow Canyon is shown as an example in the inset.

alluvium remains confined to the valley up to at least 19200 years. Instead, a hanging valley, or waterfall appears at the canyon-fan transition (Crosby et al., 2007). This feature likely relaxes to sub-vertical and migrates upstream (Scheingross et al., 2020), but relevant mechanics are not included here. Such a waterfall, Darwin Falls, is seen two canyons south of Rainbow Canyon (inset of Figure 5b). It is located about 5 km upstream of the mouth, and forms a waterfall due to a permanent spring. Raming and Whipple (2022) have shown how such a feature can prevent the immediate upstream transmission of base level fall, in this case induced by a high rate of production of accommodation in the valley. Upstream of the waterfall in Figure 5b, incision and uplift continue to balance. This example demonstrates how canyon and fan can fail to communicate with each other.

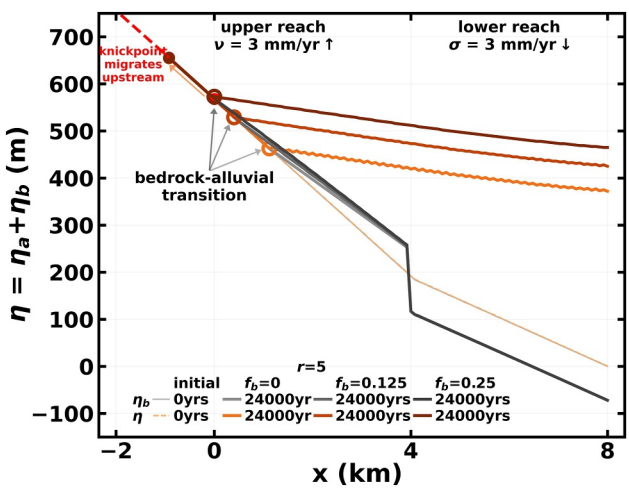

Figure 6. Illustration of the effect of sediment supply from the canyon sidewalls. Calculational conditions are the same as Figure 4a ($\sigma = v = E = 3$ mm/year), and the same wide valley ($r = 5$), however with three different sidewall feed rates corresponding to $f_b = 0$, 0.125, and 0.25.

Figure 6 is a variant of Figure 4a, with the same run conditions as that figure but with the sidewall sediment input factor f_b taking the values 0. 0.125, and 0.25. Increasing sidewall input pushes both the position of the bedrock-alluvial transition upstream and the corresponding elevation higher.

Several variant cases are shown in the Figures in Supporting Information S1. Figure S1 in Supporting Information S1 corresponds to Figures 3a and 3b but considers pure incision with E balancing $v = 3$ mm/year in the upper reach. Nothing happens in that reach except upstream migration of the knickpoint. Figure S2 in Supporting Information S1 corresponds to Figure 4a, but with punctuated uplift every 240 years rather than continuous uplift. Little difference is seen at sufficiently large time and space scales.

Figure S3 in Supporting Information S1 shows the effect of heavy sidewall sediment input for 6000 years, with the value $f_b = 0.5$, and a reduction in the upstream sediment feed rate to 1/100 beyond that time. The figure illustrates the ability of the model to capture multiple interacting drivers.

5. Discussion

We bring together in a simplified way tectonics, sediment transport, alluviation, incision and bed morphodynamics to link erosional and depositional processes in a canyon-fan system. This linkage advances the study of geomorphology at source-to-sink scale.

21699011, 2026, 6, Downloaded from https://agupubs.onlinelibrary.wiley.com/doi/10.1029/2025JF008718 by Texas Tech University Libraries, Wiley Online Library on [30/09/2026]. See the Terms and Conditions (https://onlinelibrary.wiley.com/terms-and-conditions) on Wiley Online Library for rules of use; OA articles are governed by the applicable Creative Commons License

21699011, 2026, 6, Downloaded from https://agupubs.onlinelibrary.wiley.com/doi/10.1029/2025JF008718 by Texas Tech University Libraries, Wiley Online Library on [30/09/2026]. See the Terms and Conditions (https://onlinelibrary.wiley.com/terms-and-conditions) on Wiley Online Library for rules of use; OA articles are governed by the applicable Creative Commons License

Our model is "1.5 D" (1D with extension to canyon sidewall erosion and channel migration on the fan). In this sense, it is less complex than 2D cellular models (Densmore et al., 2007; Pepin et al., 2010; Welivitiya et al., 2020). It does, however, include relations for sediment transport, cover and incision that have a strong basis in experimental and field research. It allows specific insight into canyon-fan interaction and migration of a bedrock-alluvial transition.

The effect of climate change could be included in part by changing the flood discharge and intermittency. Based on the results for punctuated uplift in Figure S2 of Supporting Information S1, the model would not likely show a clear signal for cyclic climate change over hundreds of years. Changes in flood discharge and intermittency corresponding to inferred records of climate change over a glacial cycle would give rise to a signal. Death Valley itself is often partially or fully occupied by Lake Manly, especially during glacial periods. Lake Manly had highstands approximately 26,000, 18,000 and 12,000 years before present (Hershler et al., 1999), and Panamint Valley was similarly occupied by Panamint Lake (Jayko et al., 2008). Under such circumstances, the model used to model the bajada (line fan) can be altered in a straightforward way to describe a line fan-delta (Kostic & Parker, 2003) that responds to rise and fall of the lake level (Parker et al., 2008b).

Our analysis indicates that a bedrock-alluvial transition can be present within the canyon itself even when the plateau into which the canyon is incised is actively uplifting. One possible counterargument to the above conclusions is that the Rainbow Canyon/Panamint Valley region is tectonically dead and may have been so for tens of thousands of years. According to this argument, the presence of a bedrock-alluvial transition partway up the canyon may simply represent onlapping since the cessation of tectonics. Three arguments suggest that this alternative conclusion may not be general. (a) Labotka and Albee (1990) estimate the following for the Panamint Range: "The 120 m of uplift was attained since about 40,000 B.P." (b) The same reference notes as follows: "Present uplift is occurring along the Panamint Valley fault zone." (c) Figures 3c and 3d suggests that in the absence of tectonics, sediment might have overflowed the canyon and spilled out onto the Darwin Plateau in a matter of a few thousand years.

The figures above often show mild but stable oscillations in bed elevation η. These are most likely a result of our rather simple numerical method, including a first-order Euler step method for the time derivative and a similar first-order method for spatial derivatives. A numerical method of higher order accuracy would subdue or eliminate these oscillations.

The analysis presented here indicates the possibility of a bedrock interface buried deep below an alluvial cover in a canyon. Hsu et al. (2010) report on an electrical resistivity imaging method that could be used to detect such interfaces.

6. Conclusions

We present a morphodynamic model of an interacting canyon and fan which captures the dynamics of a bedrock-alluvial transition bounding the two. The basis for the model is a unified approach to sediment transport and conservation which captures both partial and complete alluviation, bedrock incision, knickpoint migration and basement tectonics. As opposed to most treatments based on the stream power model, sediment continuity is satisfied everywhere. Three novel results proceed from the above analysis.

1. In a linked canyon-fan system, the canyon and fan can communicate with each other, in the sense that even when the canyon undergoes uplift, alluviation from downstream can push the bedrock-alluvial transition well into the canyon itself. This alluviation "turns off" incision by burying the bedrock, so that uplift there reduces the accommodation for alluvium and pushes the transition even faster up the canyon (Figure 4a).
2. When competent sediment delivered from canyon sidewalls is excluded, a set of conditions exist whereby at any given time (within some range) the streamwise position of the bedrock-alluvial transition in the canyon displaces downstream with increasing uplift rate, but the elevation of that point remains invariant (Figures 4d and 5a).
3. When the valley is sufficiently wide compared with the canyon, however, alluvium may not onlap the canyon bedrock for long periods of time, and instead a hanging valley, or vertical face forms at the canyon mouth (Figure 5b).

21699011, 2026, 6, Downloaded from https://agupubs.onlinelibrary.wiley.com/doi/10.1029/2025JF008718 by Texas Tech University Libraries, Wiley Online Library on [30/09/2026]. See the Terms and Conditions (https://onlinelibrary.wiley.com/terms-and-conditions) on Wiley Online Library for rules of use; OA articles are governed by the applicable Creative Commons License

These results strictly apply only under the simplified formulation and constraints of the present model. Future extensions of the model can help determine to what degree they generalize to the complex setting presented by Basin and Range tectonics.

Conflict of Interest

The authors declare no conflicts of interest relevant to this study.

Availability Statement

All data used herein are included in the main text. The software used in the calculations consists of Python code are available on Zenodo at the link: https://doi.org/10.5281/zenodo.18490840 (Zhang, 2026). The software is not licensed and can be accessed without registration.

Acknowledgments
We acknowledge funding from: the National Natural Science Foundation of China 52109092 and 52579064 (LZ) and U2340204; the China Fundamental Research Funds for Central Universities 2023MS070 (LZ); and the W.H. Johnson Chair of the Department of Earth Science and Environmental Change, University of Illinois Urbana-Champaign (GP). We thank Aaron Yoshinobu, Suzanne Anderson and Kelin Whipple for their helpful comments and advice, and Takuya Inoue for useful edits and comments.

References

Blair, T. C., & McPherson, J. G. (2009). Chapter 14: Processes and forms of Alluvial Fans. In *Geomorphology of desert environments* (pp. 413–467). Springer.

Burchfiel, B. C., Molnar, P., Zhang, P., Deng, Q., Zhang, W., & Wang, Y. (1994). Example of a supradetachment basin within a pull-apart tectonic setting: Mormon Point, Death Valley, California. *Basin Research*, *7*(2), 199–214. https://doi.org/10.1111/j.1365-2117.1995.tb00104.x

Chatanantavet, P., & Parker, G. (2008). Experimental study of bedrock channel alluviation under varied sediment supply and hydraulic conditions. *Water Resources Research*, *44*(12), W12446. https://doi.org/10.1029/2007WR006581

Chatanantavet, P., & Parker, G. (2009). Physically based modeling of bedrock incision by abrasion, plucking, and macroabrasion. *Journal of Geophysical Research*, *114*(F4), F04018. https://doi.org/10.1029/2008JF001044

Cichanski, M. (2000). Low-angle, range-flank faults in the Panamint, Inyo, and Slate ranges, California: Implications for recent tectonics of the Death Valley region. *Geological Society of America Bulletin*, *112*(6), 871–883. https://doi.org/10.1130/0016-7606(2000)112<0871:larffi>2.3.co;2

Crosby, B. T., Whipple, K. X., Gasparini, N. M., & Wobus, C. W. (2007). Formation of fluvial hanging valleys: Theory and simulation. *J. Geophys. Res.Earth Surface*, *112*(F3), F03S10. https://doi.org/10.1029/2006JF000566

Densmore, A. L., Allen, P. A., & Simpson, G. (2007). Development and response of a coupled catchment fan system under changing tectonic and climatic forcing. *Journal of Geophysical Research*, *112*(F1), F01002. https://doi.org/10.1029/2006jf000474

Gasparini, N. M., & Brandon, M. (2011). A generalized power law approximation for fluvial incision of bedrock channels. *J. Geophys. Res.Earth Surface*, *116*(F2), F02020. https://doi.org/10.1029/2009JF001655

Hershler, R., Mulvey, M., & Liu, H. P. (1999). Biogeography in the Death Valley region: Evidence from springsnails (Hydrobiidae: Tryonia). *Zoological Journal of the Linnean Society*, *126*(3), 335–354. https://doi.org/10.1111/j.1096-3642.1999.tb01375.x

Howard, A. D. (1994). A detachment-limited model of drainage basin evolution. *Water Resources Research*, *30*(7), 2261–2285. https://doi.org/10.1029/94wr00757

Hsu, H. L., Yanites, B. J., Chen, C. C., & Chen, Y. G. (2010). Bedrock detection using 2D electrical resistivity imaging along the Peikang River, central Taiwan. *Geomorphology*, *114*(3), 406–414. https://doi.org/10.1016/j.geomorph.2009.08.004

Hupp, C. R. (2000). Hydrology, geomorphology and vegetation of Coastal Plain rivers in the south-eastern USA. *Hydrological Processes*, *14*(16–17), 2991–3010. https://doi.org/10.1002/1099-1085(200011/12)14:16/17<2991::aid-hyp131>3.0.co;2-h

Jafarinik, S., & Viparelli, E. (2020). Alluvial morphodynamics of low-slope bedrock reaches transporting nonuniform bed material. *Water Resources Research*, *56*(10), e2020WR027345. https://doi.org/10.1029/2020wr027345

Jayko, A. S., Forester, R., Kaufman, D., Phillips, F., Yount, J., McGeehin, J., & Mahan, S. (2008). Late Pleistocene lakes and wetlands, Panamint Valley, Inyo County, California. In *Late Cenozoic drainage history of the Southwestern great Basin and lower Colorado River Region: Geologic and biotic perspectives* (Vol. 439, pp. 151–184). Geological Society of America Special Paper. https://doi.org/10.1130/2008.2439(07)

Kim, W., & Muto, T. (2007). Autogenic response of alluvial-bedrock transition to base-level variation: Experiment and theory. *Journal of Geophysical Research: Earth Surface*, *112*(F3), F03S14. https://doi.org/10.1029/2006JF000561

Kim, Y., Kim, W., Cheong, D., Muto, T., & Pyles, D. R. (2013). Piping coarse-grained sediment to a deep water fan through a shelf-edge delta bypass channel: Tank experiments. *Journal of Geophysical Research*, *118*(4), 2279–2291. https://doi.org/10.1002/2013jf002813

Kostic, S., & Parker, G. (2003). Progradational sand-mud deltas in lakes and reservoirs. Part 1. Theory and numerical modeling. *Journal of Hydraulic Research*, *41*(2), 127–140. https://doi.org/10.1080/00221680309499956

Labotka, T. C., & Albee, A. L. (1990). Chapter 17: Uplift and exposure of the Panamint metamorphic complex, California. In *Basin and range extensional tectonics near the latitude of Las Vegas, Nevada* (pp. 345–362). Geological Society of America.

Lague, D. (2014). The stream power river incision model: Evidence, theory and beyond. *Earth Surface Processes and Landforms*, *39*(1), 38–61. https://doi.org/10.1002/esp.3462

Muto, T. (2001). Shoreline autoretreat substantiated in flume experiment. *Journal of Sedimentary Research*, *71*(2), 246–254. https://doi.org/10.1306/091400710246

Muto, T., & Steel, R. J. (2001). Autostepping during the transgressive growth of deltas: Results from a flume experiment. *Geology*, *29*(9), 771–774. https://doi.org/10.1130/0091-7613(2001)029<0771:adttgo>2.0.co;2

Nucci, A., Angiolini, C., Landi, M., & Bacchetta, G. (2012). Influence of bedrock-alluvial transition on plant species distribution along a Mediterranean river corridor. *Plant Biosystems*, *146*(3), 564–575.

Parker, G., et al. (1998b). Alluvial fans formed by channelized fluvial and sheet flow: Application. *Journal of Hydraulic Engineering*, *124*(10), 12–20.

Parker, G., Muto, T., Akamatsu, Y., Dietrich, W. E., & Lauer, J. W. (2008a). Unraveling the conundrum of river response to rising sea level: From laboratory to field. Part I. Laboratory experiments. *Sedimentology*, *55*(6), 1643–1655. https://doi.org/10.1111/j.1365-3091.2008.00961.x

Parker, G., Muto, T., Akamatsu, Y., Dietrich, W. E., & Lauer, J. W. (2008b). Unraveling the conundrum of river response to rising sea level: From laboratory to field. Part II. The fly-Strickland River System, Papua New Guinea. *Sedimentology*, *55*(6), 1657–1688.

Parker, G., Paola, C., Whipple, K., & Mohrig, D. (1998). Alluvial fans formed by channelized fluvial and sheet flow: Theory. *Journal of Hydraulic Engineering*, *124*(10), 1–11.

Pavich, M. J. (1989). Regolith residence time and the concept of surface age of the piedmont "Peneplain". *Geomorphology*, *2*(1–3), 181–196. https://doi.org/10.1016/0169-555x(89)90011-1

Pepin, E., Carretier, S., & Herail, G. (2010). Erosion dynamics modelling in a coupled catchment-fan system with constant external forcing. *Geomorphology*, *122*(1–2), 78–90. https://doi.org/10.1016/j.geomorph.2010.04.029

Raming, L. W., & Whipple, K. X. (2022). When knickzones limit upstream transmission of base-level fall: An example from Kaua'i, Hawai'i. *Geology*, *50*(12), 382–1386. https://doi.org/10.1130/g50019.1

Scheingross, J. S., & Lamb, M. P. (2017). A mechanistic model of knickpoint plunge pool erosion into bedrock. *Journal of Geophysical Research: Earth Surface*, *122*(11), 2079–2104. https://doi.org/10.1002/2017jf004195

Scheingross, J. S., Lamb, M. P., & Fuller, B. M. (2019). Self formed bedrock knickpoints. *Nature*, *567*(7747), 229–233. https://doi.org/10.1038/s41586-019-0991-z

Scheingross, J. S., Limaye, A. B., McCoy, S. W., & Whittaker, A. C. (2020). The shaping of erosional landscapes by internal dynamics. *Nature Reviews Earth & Environment*, *1*(12), 661–676. https://doi.org/10.1038/s43017-020-0096-0

Sklar, L. S., & Dietrich, W. E. (2004). A mechanistic model for river incision into bedrock by saltating bed load. *Water Resources Research*, *40*(6), W06301. https://doi.org/10.1029/2003wr002496

Sklar, L. S., & Dietrich, W. E. (2006). The role of sediment in controlling steady-state bedrock channel slope: Implications of the saltation-abrasion incision model. *Geomorphology*, *82*(1–2), 58–83. https://doi.org/10.1016/j.geomorph.2005.08.019

Stewart, J. H. (1971). Basin and range structure: A system of horsts and grabens produced by deep-seated extension. *Geological Society of America Bulletin*, *82*(4), 1019–1044. https://doi.org/10.1130/0016-7606(1971)82[1019:barsas]2.0.co;2

Sun, T., Paola, C., Parker, G., & Meakin, P. (2002). Fluvial fan-deltas: Linking channel processes with large-scale morphodynamics. *Water Resources Research*, *38*(8). https://doi.org/10.1029/2001WR000284

Sun, Y., Gu, Z. G., Ma, J., & Yi, X. Y. (2022). Experimental study on formation characteristics and influence of ice jam in melting period. *Journal of Physics: Conference Series*, *2271*(1), 012009. https://doi.org/10.1088/1742-6596/2271/1/012009

Turowski, J. M., D. Lague, D., & Hovius, N. (2007). Cover effect in bedrock abrasion: A new derivation and its implications for the modeling of bedrock channel morphology. *Journal of Geophysical Research: Earth Surface*, *112*(F4), F04006. https://doi.org/10.1029/2006JF000697

Viparelli, E., Nittrouer, J. A., & Parker, G. (2015). Modeling flow and sediment transport dynamics in the lowermost Mississippi River, Louisiana, USA, with an upstream alluvial-bedrock transition and a downstream bedrock-alluvial transition: Implications for land building using engineered diversions. *Journal of Geophysical Research*, *120*(3), 534–563. https://doi.org/10.1002/2014jf003257

Waskiewicz, T., Mihir, M., & Whitworth, J. (2008). Surface variability of alluvial fans generated by disparate processes, eastern Death Valley, CA. *The Professional Geographer*, *60*(2), 207–223.

Welivitiya, W. D. D. P., Willgoose, G. R., & Hancock, G. R. (2020). Geomorphological evolution and sediment stratigraphy of numerically simulated alluvial fans. *Earth Surface Processes and Landforms*, *45*(9), 2148–2166. https://doi.org/10.1002/esp.4872

Whipple, K. X., Parker, G., Paola, C., & Mohrig, D. (1998). Channel dynamics, sediment transport, and the slope of alluvial fans: Experimental Study. *Journal of Geology*, *106*(6), 677–693. https://doi.org/10.1086/516053

Whipple, K. X., & Tucker, G. E. (1999). Dynamics of the stream-power river incision model: Implications for height limits of mountain ranges, landscape response timescales, and research needs. *Journal of Geophysical Research*, *104*(B8), 17661–17674. https://doi.org/10.1029/1999jb900120

Windley, B. F., & Allen, M. B. (1993). Mongolian plateau: Evidence for a late Cenozoic mantle plume under central Asia. *Geology*, *21*(4), 295–298. https://doi.org/10.1130/0091-7613(1993)021<0295:mpefal>2.3.co;2

Zhang, L. (2026). lizhangpig/Panamint-Canyon-Fan: Panamint-canyon-fan (V1.0 (V1.0)) [Software]. *Zenodo*. https://doi.org/10.5281/zenodo.18490840

Zhang, L., Li, T. J., Wang, G. Q., Nittrouer, J. A., Parker, G., & Fu, X. (2020). How canyons evolve by incision into bedrock: Rainbow Canyon, Death Valley National Park, USA. *Proceedings of the National Academy of Sciences of the United States of America*, *117*(26), 14730–14737. https://doi.org/10.1073/pnas.1911040117

Zhang, L., Parker, G., Stark, C. P., Inoue, T., Viparelli, E., Fu, X., & Izumi, N. (2015). Macro-roughness model of bedrock-alluvial river morphodynamics. *Earth Surface Dynamics*, *3*(1), 113–138. https://doi.org/10.5194/esurf-3-113-2015

Zhang, L., Stark, C. P., Schumer, S., Fu, X. D., Kwang, J., Li, T. J., & Parker, G. (2018). The advective-diffusive morphodynamics of mixed bedrock-alluvial rivers subjected to spatiotemporally varying sediment supply. *J. Geophys. Res.Earth Surface*, *123*(8), 1731–1755. https://doi.org/10.1029/2017jf004431

Zhou, J. P., Li, S., Liu, Y., Liu, B., Li, W., Wang, G., et al. (2023). Differential uplift triggered basin-and-range system: Evidence from low-temperature thermochronology in Eastern NE Asia. *Tectonics*, *43*(1), e2023TC007857. https://doi.org/10.1029/2023tc007857

21699011, 2026, 6, Downloaded from https://agupubs.onlinelibrary.wiley.com/doi/10.1029/2025JF008718 by Texas Tech University Libraries, Wiley Online Library on [30/09/2026]. See the Terms and Conditions (https://onlinelibrary.wiley.com/terms-and-conditions) on Wiley Online Library for rules of use; OA articles are governed by the applicable Creative Commons License